

A molecular redox switch *via* iron translocation in a bicompartamental ligand

Catherine Belle,^a Jean-Louis Pierre^{*a} and Eric Saint-Aman^b

^a Laboratoire de Chimie Biomimétique (LEDSS, CNRS UMR 5616)

^b Laboratoire d'Electrochimie Organique et de Photochimie Redox (LEOPR, CNRS UMR 5630), Université J. Fourier, BP 53, 38041 Grenoble cedex 9, France

Mononuclear complexes of an unsymmetrical bicompartamental ligand containing an iron ion that can occupy either the 'soft nitrogen box' or the 'hard oxygen box' have been synthesized. When the ferric iron is electrochemically reduced or when the ferrous iron is electrochemically oxidized, it hops from one binding site to the other. The process is reversible. During the switching process, the iron ion remains bound to the bridging phenolate ligand and the iron translocation may be regarded as a 'pendular motion'.

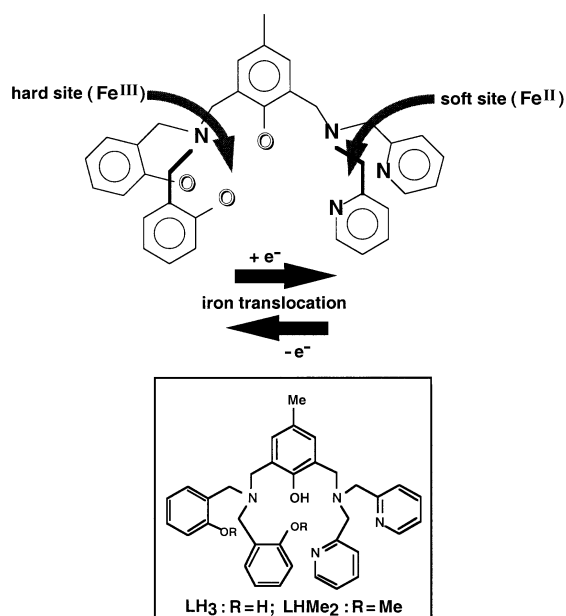
Un interrupteur moléculaire par translocation du fer dans un ligand à deux compartiments. Des complexes mononucléaires d'un ligand à deux compartiments dissymétriques contenant un ion fer qui peut occuper soit le compartiment azoté (mou), soit le compartiment oxygéné (dur) ont été préparés. Quand l'ion ferrique est réduit électrochimiquement ou quand l'ion ferreux est oxydé électrochimiquement, il saute d'un compartiment à l'autre. Le processus est réversible. Pendant la translocation, le métal reste lié au groupement phénolate pontant, dans un mouvement pendulaire.

The vision of molecule-based technology has motivated fascinating work from many research teams. The realization of molecular switches may further the progress of miniaturization of electronic circuits.¹ Moreover, biological switches play a paramount role in controlling cellular processes. Molecular switches have been recently described that respond reversibly to various external triggers (photons, protons or electrons^{2–4}). In an outstanding report, Shanzer and colleagues² have shown that it is possible to build a molecular switch involving the translocation of a metal ion, operated by the gain or loss of an electron. In other examples of redox switches, the trigger displaces one or two arms of the ligand (and not the metal atom itself).^{3,4} A redox switch can be based on a ligand system containing both hard and soft binding sites. A single metal atom is expected to bind specifically to one or the other site, depending on its oxidation state. By modifying the oxidation state, the metal ion is expected to translocate intramolecularly from one site to the other (Scheme 1). In the Shanzer switches, the reversible translocation of an iron ion between the two sites was achieved by chemical oxidation and reduction. We present here a redox switch based on an unsymmetrical bicompartamental ligand, LH₃⁵ (Scheme 1), in which the reversible positional change of an iron ion is electrochemically controlled, allowing a direct chemical transformation of energy into controlled oriented motion at a molecular level. Some examples of electrochemically induced molecular hysteresis⁶ have been demonstrated.^{7,8} The electrochemically triggered swinging of a [2]-catenate⁹ and an electrochemically switched anion translocation in a multicomponent coordination compound¹⁰ have been evidenced. The originality of the ligand LH₃ arises from the bridging phenolate group, which may remain coordinated with the two redox states of the iron atom, thus favouring intramolecular translocation *via* a 'pendular motion' of the metal ion *versus* an exchange process involving a decomplexation–complexation mechanism.

Results and Discussion

Iron complexes

Only mononuclear complexes have been obtained by the experimental procedures described here. Iron dinuclear complexes from LH₃ had been previously described by us.¹¹ The redox processes have been studied with the complexes obtained in the absence or in the presence of collidine (a base can aid the control of the protonation-deprotonation of the phenolic ligands). For the mononuclear Fe^{III} complex from LH₃, the iron ion is in the 'oxygen box' (hard site in Scheme 1). This is unambiguously demonstrated by the spectrum of the Fe^{III} complex of LHMe₂ in which the 'oxygen box' has been suppressed, forcing the iron ion to be in the 'nitrogen



Scheme 1 Schematic representation of the redox switch using LH₃

* E-mail: Jean-Louis.Pierre@ujf-grenoble.fr

box'. The observation of a phenolate-to-iron LMCT band in the ferric complex of LHMe_2 shows that the iron located in the 'nitrogen box' is coordinated by the phenolate bridging group. For the mononuclear Fe^{II} complexes, the iron ion is in the 'nitrogen box'. This is corroborated by the similar spectra observed for the complexes from LH_3 and LHMe_2 , respectively. The results are in accordance with the 'Hard and Soft Acids and Bases' principle. They are also in accordance with the redox studies (*vide infra*).

Electrochemistry

The cyclic voltammetry (CV) curve of the $[\text{Fe}^{\text{II}}, \text{LHMe}_2\text{-N}_3\text{O}]^{\dagger}$ complex in neutral CH_3CN electrolyte displays a reversible redox wave at $E_{1/2} = 0.28 \text{ V}$ ($\Delta E_p = 80 \text{ mV}$, $v = 0.1 \text{ V s}^{-1}$) corresponding to the $\text{Fe}^{\text{II}}/\text{Fe}^{\text{III}}$ redox couple [Fig. 1(A)]. This is confirmed by the voltammogram at the platinum RDE (rotating disc electrode), which exhibits a well-behaved redox wave [Fig. 1(B)] at $E_{1/2} = 0.28 \text{ V}$. Coulometric titration confirmed a one-electron transfer. Starting from a solution containing stoichiometric amounts of LHMe_2 and $\text{Fe}(\text{ClO}_4)_3$, the same general behaviour has been observed. However, an additional weak electrochemical signal is observed on the CV [Fig. 1(C)] or RDE curves ($E_p = -0.43 \text{ V}$ and $E_{1/2} = -0.44 \text{ V}$, respectively) showing that the $[\text{Fe}^{\text{III}}, \text{LHMe}_2\text{-N}_3\text{O}]$ complex can be quantitatively produced only by exhaustive electrochemical oxidation of the corresponding $[\text{Fe}^{\text{II}}, \text{LHMe}_2\text{-N}_3\text{O}]$ complex.

The CV curve of the $[\text{Fe}^{\text{II}}, \text{LH}_3\text{-N}_3\text{O}]$ complex in neutral CH_3CN electrolyte is characterized by a quasi-reversible

anodic oxidation peak at $E_p = 0.31 \text{ V}$. On the reverse scan, the corresponding cathodic process is seen at $E_p = 0.20 \text{ V}$ ($\Delta E_p = 0.11 \text{ V}$; $v = 0.1 \text{ V s}^{-1}$) in addition to an extra cathodic process at $E_p = -0.07 \text{ V}$ [Fig. 2(A)]. The stationary voltammogram at the platinum RDE of the $[\text{Fe}^{\text{II}}, \text{LH}_3\text{-N}_3\text{O}]$ electrochemical solution displays a wave at $E_{1/2} = 0.26 \text{ V}$ [Fig. 2(B)]. After exhaustive electrolysis (one exchanged electron), the voltammogram exhibits two successive cathodic waves [Fig. 2(C)] at $E_{1/2} = 0.26$ and -0.11 V , respectively, having similar intensities. Further reduction of the one-electron oxidized solution restores fully the original voltammogram. The same electrochemical features have been found starting from a solution containing a stoichiometric mixture of LH_3 and $\text{Fe}(\text{ClO}_4)_3$. These findings indicate that the $[\text{Fe}^{\text{II}}, \text{LH}_3\text{-N}_3\text{O}]$ complex leads to two different species upon oxidation. The first one, characterized by $E_{1/2} = 0.26 \text{ V}$, is the corresponding $[\text{Fe}^{\text{III}}, \text{LH}_3\text{-N}_3\text{O}]$ complex, as judged by the reversibility of the electron transfer process. The second one is characterized by an irreversible reduction at $E_{1/2} = -0.11 \text{ V}$, restoring the initial $[\text{Fe}^{\text{II}}, \text{LH}_3\text{-N}_3\text{O}]$ complex upon exhaustive reduction. This indicates a reversible change in the coordination sphere of the iron centre and suggests a partial reversible translocation of the iron atom during the electron transfer through an intramolecular motion leading to the stable $[\text{Fe}^{\text{III}}, \text{LH}_3\text{-NO}_3]$ complex.

Comparison of the results obtained with LHMe_2 and LH_3 corroborates the finding that in the $\text{LH}_3 + \text{Fe}^{\text{II}}$ complex, the Fe^{II} ion is coordinated by the pyridine ligands: the formal potentials of the $\text{LHMe}_2 + \text{Fe}^{\text{II}}/\text{Fe}^{\text{III}}$ and $\text{LH}_3 + \text{Fe}^{\text{II}}/\text{Fe}^{\text{III}}$ redox couples are very close and LHMe_2 provides only pyridine pendant arms as coordinating sites. Thus, the electrochemical process undergone by the $\text{LH}_3 + \text{Fe}^{\text{II}}/\text{Fe}^{\text{III}}$ system can be schematized as shown in Scheme 2.

Since the coordination of Fe^{III} by the phenolic moieties of LH_3 is accompanied by the release of protons, it could be assumed that the equilibrium between the two Fe^{III} complexes shown in Scheme 2 is displaced in basic medium towards the complex in which the iron ion is coordinated to the phenolate groups. The electrochemical behaviour of the $\text{LH}_3 + \text{Fe}^{\text{II}}/\text{Fe}^{\text{III}}$ redox couple has thus been studied in the presence of collidine. The CV curve [Fig. 3(A)] exhibits an irreversible anodic peak at $E_p = -0.18 \text{ V}$, the corresponding cathodic process occurs at $E_p = -0.65 \text{ V}$. The voltammograms at the plati-

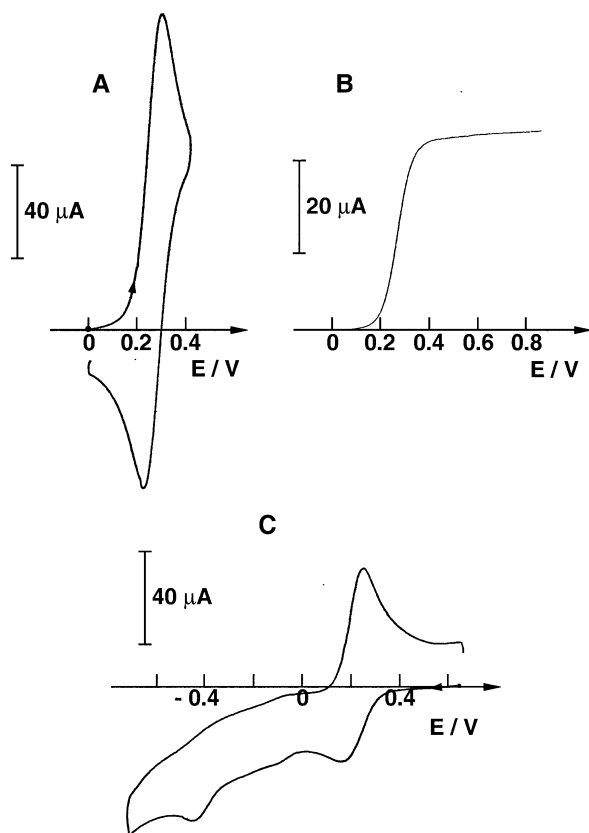


Fig. 1 (A) Cyclic voltammogram of $\text{LHMe}_2 + \text{Fe}^{\text{II}}$ (4.0 mM) at a Pt disc (5 mm diameter); scan rate: 0.1 V s^{-1} . (B) Voltammogram of $\text{LHMe}_2 + \text{Fe}^{\text{II}}$ (4.0 mM) at a Pt RDE (2 mm diameter, $N = 600 \text{ rpm}$). (C) Cyclic voltammogram of $\text{LHMe}_2 + \text{Fe}^{\text{III}}$ (1.5 mM) at a Pt disc (5 mm diameter); scan rate: 0.1 V s^{-1} . Electrolyte: $\text{CH}_3\text{CN} + 0.1 \text{ M TBAP}$. E vs. $\text{Ag}/10 \text{ mM AgNO}_3 + \text{CH}_3\text{CN} + 0.1 \text{ M TBAP}$

\dagger In brackets is indicated the ligand followed by the nature of the coordination sphere in order to specify the bonding mode.

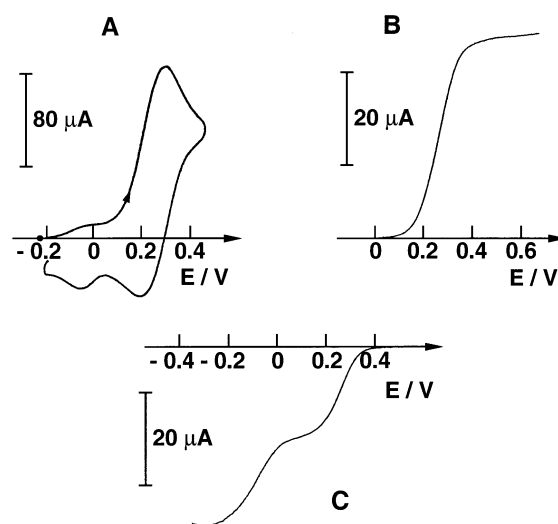
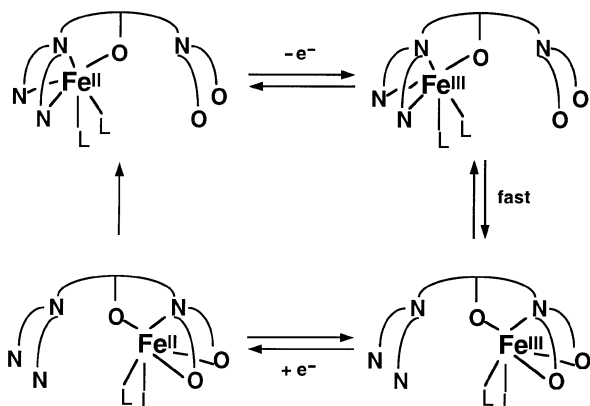


Fig. 2 (A) Cyclic voltammogram of $\text{LH}_3 + \text{Fe}^{\text{II}}$ (4.0 mM) at a Pt disc (5 mm diameter); scan rate: 0.1 V s^{-1} . (B) Voltammogram of $\text{LH}_3 + \text{Fe}^{\text{II}}$ (4.0 mM) at a Pt RDE (2 mm diameter, $N = 600 \text{ rpm}$). (C) Voltammogram after exhaustive electrolysis at 0.5 V ($n = 1 \text{ e}^-$) of $\text{LH}_3 + \text{Fe}^{\text{II}}$ (4.0 mM) at a Pt RDE (2 mm diameter, $N = 600 \text{ rpm}$). Electrolyte: $\text{CH}_3\text{CN} + 0.1 \text{ M TBAP}$. E vs. $\text{Ag}/10 \text{ mM AgNO}_3 + \text{CH}_3\text{CN} + 0.1 \text{ M TBAP}$



Scheme 2 The electrochemical mechanism for the $\text{LH}_3 + \text{Fe}^{\text{II}}/\text{Fe}^{\text{III}}$ system

num RDE for the $\text{LH}_3 + \text{Fe}^{\text{II}}$ [Fig. 3(B)] and $\text{LH}_3 + \text{Fe}^{\text{III}}$ [Fig. 3(C)] CH_3CN electrochemical solutions in the presence of collidine show an anodic wave at $E_{1/2} = -0.26$ V and a cathodic wave at $E_{1/2} = -0.68$ V, respectively. Therefore, oxidation and reduction processes take place at different potentials ($\Delta E_{1/2} = 0.42$ V), indicating a change in the coordination sphere around the iron centre upon electron transfer.^{12,13} When two Fe^{III} complexes are obtained from the ferrous complex in the absence of added base, addition of collidine allows the obtention of one ferric complex as judged by the observation of one cathodic peak on the CV curve: the base facilitates the deprotonation of the phenolic groups. It must be emphasized that starting from the Fe^{II} or Fe^{III} complex, the same CV features have been found, showing that the change is chemically reversible on the CV timescale. Analysis of the CV curves as a function of the scan rate¹⁴ according to the electrochemical mechanism proposed on Scheme 2 shows that the rate constant, k , of the translocation process obeys $\log(k/\text{s}^{-1}) > 2$.

The possibility to translocate affects the redox potentials drastically. The reduction potential of the ferric iron maintained in the 'oxygen box' of a diferric complex of LH_3 is

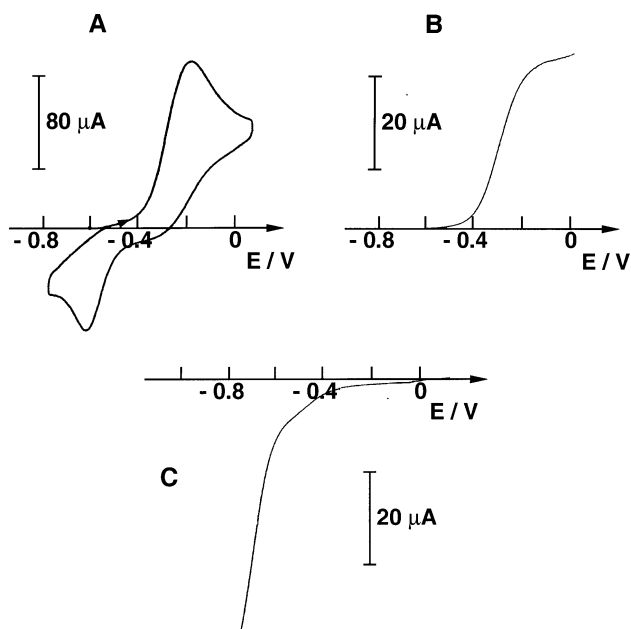


Fig. 3 (A) Cyclic voltammogram of $\text{LH}_3 + \text{Fe}^{\text{II}}$ (4.0 mM) at a Pt disc (5 mm diameter) in the presence of one molar equivalent of collidine; scan rate: 0.1 V s^{-1} . (B) Voltammogram of $\text{LH}_3 + \text{Fe}^{\text{II}}$ (4.0 mM) at a Pt RDE (2 mm diameter, $N = 600$ rpm) in the presence of one molar equivalent of collidine. (C) Voltammogram of $\text{LH}_3 + \text{Fe}^{\text{III}}$ (7.2 mM) at a Pt RDE (2 mm diameter, $N = 600$ rpm) in the presence of one molar equivalent of collidine. Electrolyte: $\text{CH}_3\text{CN} + 0.1 \text{ M TBAP}$. E vs. $\text{Ag}/10 \text{ mM AgNO}_3 + \text{CH}_3\text{CN} + 0.1 \text{ M TBAP}$

-1.29 V .¹¹ In the mononuclear complex of LH_3 , the reduction of the Fe^{III} centre takes place at -0.68 V (in the presence of collidine), the metal cation being able to translocate from the 'oxygen box' to the 'nitrogen box'. The oxidation potential of the ferrous iron maintained in the 'nitrogen box' is 0.33 V (LHMe_2 in the presence of collidine) and it is -0.26 V when it can translocate from the 'nitrogen box' to the 'oxygen box'. Reciprocally, this type of change in redox potentials can be used as proof of a translocation process.

Spectroscopic studies of the electrochemical solutions

Electrochemical one-electron reduction of all the ferric complexes causes the appearance of new UV/VIS spectral features. The reversibility of the process is further demonstrated considering that, on re-oxidation, the original $\text{LH}_3 + \text{Fe}^{\text{III}}$ spectra are recovered. In addition, the spectroscopic UV/VIS features from oxidized $\text{LH}_3 + \text{Fe}^{\text{II}}$ complexes are identical with those of $\text{LH}_3 + \text{Fe}^{\text{III}}$ complexes obtained by treatment of the ligands with $\text{Fe}(\text{ClO}_4)_3$ (1 equiv.). The same reversibility in the UV/VIS spectral features has been found considering the ferrous complex obtained electrolytically from an electrolytic solution of the ferric complex or by treatment of the ligands with $\text{Fe}(\text{ClO}_4)_2$ (1 equiv., see experimental). The EPR spectra of the oxidized solutions at 70 K (high-spin Fe^{III} with $g = 4.3$) are identical to those of the $\text{LH}_3 + \text{Fe}^{\text{III}}$ complexes.

Experimental

Materials and methods

Commercial reagents (from Aldrich) were used as obtained without further purification. Solvents were purified by standard methods before use. Collidine was distilled and stored on potassium hydroxide.

Caution: Although no problems were encountered, suitable care and precautions should be taken when handling the perchlorate salts.

Spectrometry. Fast-atom bombardment (FAB) mass spectra in the positive ion mode were recorded on a Nermag R 1010C apparatus equipped with a M scan (Wallis) atom gun (8 kV, 20 mA). EPR spectra were recorded at 70 K on a Bruker ESP 300E spectrometer operating at 9.4 GHz (X-band). UV/VIS spectra were obtained using a Uvikon 930 spectrophotometer operating in the range $200\text{--}900 \text{ nm}$ with quartz cells. λ are given in nm and ϵ are given in $\text{M}^{-1} \text{ cm}^{-1}$.

Electrochemistry. Electrochemical experiments were carried out using a PAR model 273 potentiostat equipped with a Kipp-Zonen x - y recorder. All experiments were run at room temperature under argon atmosphere. For analytical experiments, a standard three-electrode cell was used. Potentials are referenced to an $\text{Ag}/10 \text{ mM AgNO}_3$ reference electrode with 0.1 M tetrabutylammonium perchlorate (TBAP) as supporting electrolyte in acetonitrile as solvent. Platinum disc electrodes for CV (5 mm diameter) and RDE (2 mm diameter) experiments were polished with $1 \mu\text{m}$ diamond paste. A platinum plate ($2 \times 2 \text{ cm}$) was used as working electrode for electrolysis at controlled potential. The electrochemical behaviour of LH_3 and LHMe_2 has been studied in the presence of stoichiometric amounts of $\text{Fe}(\text{ClO}_4)_2$ and $\text{Fe}(\text{ClO}_4)_3$, respectively, before and after addition of collidine.

Syntheses

LH_3 . LH_3 has been prepared according to our previously described procedure.⁵ LHMe_2 was prepared by reaction of bis(2-methoxybenzyl)amine and 2-[N,N -bis(2-methylpyridyl)aminomethyl]-6-(hydroxymethyl)-4-methylphenol, prepared according to our previously described procedure.⁵

Bis(2-methoxybenzyl)amine. A mixture of 2-methoxybenzaldehyde (7.03 g, 50.6 mmol) and 2-methoxybenzylamine (7.06 g, 50.5 mmol) in 80 ml of methanol was stirred for 2 h at reflux. After cooling and slow addition of NaBH₄ (2.00 g, 52.9 mmol), the solution was stirred for 4 h at room temperature. After treatment with 30 ml of 4N HCl, the solvent was removed *in vacuo*. The solid residue was dissolved in dichloromethane, the salts were filtered off, the solution washed successively with an aqueous NaHCO₃ solution and brine, and then dried over Na₂SO₄. Evaporation of the solvent gave bis(2-methoxybenzyl)amine (12.18 g) as an oil that crystallized slowly upon standing (yield 94%). NMR (CDCl₃): ¹H (200 MHz), δ = 7.30 (m, 4H), 6.95 (m, 4H), 3.84 (s, 4H), 3.79 (s, 6H), 3.75 (s, 1H); ¹³C (50 MHz), δ = 157.5, 130.0, 128.4, 126.85, 120.4, 110.0, 55.1, 48.2.

2-[N,N-Bis(2-methylpyridyl)aminomethyl]-6-[N,N-bis(2-methoxyphenyl)aminomethyl]-4-methylphenol, LHMe₂. 2-[N,N-Bis(2-methylpyridyl)aminomethyl]-6-(hydroxymethyl)-4-methylphenol (3.61 g, 10.3 mmol) was dissolved in 70 ml of dry dichloromethane containing freshly distilled thionyl chloride (1.15 ml, 15.5 mmol). The solution was stirred at room temperature for 3 h. SOCl₂ was then distilled under reduced pressure and the product was washed several times with dry pentane to obtain a yellow powder used immediately.

A mixture prepared with NaH (1.03 g, 25 mmol, 60% in oil, washed with dry pentane) and bis(2-methoxybenzyl)amine (2.65 g, 10.3 mmol), stirred for one hour in 50 ml of dichloromethane, was added dropwise to 100 ml of dry dichloromethane containing the yellow powder obtained previously and triethylamine (2.08 ml, 15.4 mmol). Another portion of triethylamine (2.08 ml, 15.4 mmol) was then added and the mixture was kept under stirring at room temperature for two days, quenched with methanol, washed successively with an aqueous NaHCO₃ solution and brine, and then dried over Na₂SO₄. After filtration and removal of the solvent, the crude product was purified by column chromatography (neutral alumina; cyclohexane–ethyl acetate 5:1 to 1:1) to yield 4.2 g (70%) of pure LHMe₂ as a white powder (mp 112 °C). NMR (CDCl₃): ¹H (200 MHz), δ = 10.60 (br s, 1H), 8.48 (d, 2H), 7.21 (d, 4H), 7.36 (d, 2H), 7.21–6.79 (m, 10H), 3.84 (s, 4H), 3.74 (s, 6H), 3.71 (s, 2H), 3.68 (s, 2H), 3.65 (s, 4H), 2.21 (s, 3H); ¹³C (50 MHz), δ = 160.0 (Cq), 157.9 (Cq), 153.7 (Cq), 148.8 (CH), 136.2 (CH), 130.9 (CH), 129.2 (CH), 128.4 (CH), 128.2 (CH), 127.0 (Cq), 126.3 (Cq), 124.1 (Cq), 123.2 (Cq), 122.7 (CH), 121.6 (CH), 120.2 (CH), 110.2 (CH), 60.2 (CH₂), 56.1 (CH₂), 55.0 (CH₃), 52.6 (CH₂), 20.6 (CH₃). FAB-MS (positive ion mode, NBA matrix): m/z = 589 (M + H)⁺.

Fe^{II} complexes. Owing to the fact that bistability is an essential prerequisite, the preparations of the air sensitive Fe^{II} complexes were conducted in a glovebox using deaerated solvent. In 5 ml of stirred acetonitrile was added Fe(ClO₄)₂ · 6H₂O (9.1 mg, 1 equiv., 0.025 mmol) and LH₃ (14 mg, 1 equiv.). UV/VIS (CH₃CN): λ_{max} (ϵ) = 350 (sh), 600 (173). The same procedure has been used in the presence of colli-

dine; λ_{max} (ϵ) = 376 (1155). The complexes, obtained with and without collidine, from LHMe₂ exhibit the same UV/VIS spectrum with λ_{max} (ϵ) = 380 (sh) and 558 (115). Exposure of the Fe^{II} complexes to the atmosphere leads to its fast oxidation, precluding any precise chemical analysis.

Fe^{III} complexes. The same procedure was used for the Fe^{III} complexes with Fe(ClO₄)₃ · 6H₂O (11.2 mg, 0.024 mmol). The UV/VIS spectrum of the complex obtained from LH₃ without collidine exhibits λ_{max} (ϵ) = 337 (8661) and 557 (9025); FAB-MS (positive ion mode, glycerol matrix): m/z = 615 (LH₃ + Fe – H)⁺. For the complex obtained with collidine: λ_{max} (ϵ) = 380 (sh). For the complexes obtained from LHMe₂: without collidine λ_{max} (ϵ) = 303 (5131), 380 (sh) and 493 (795); with collidine FAB-MS: m/z = 743 (LHMe₂ + Fe – H + ClO₄)⁺ and 643 (LHMe₂ + Fe – H)⁺; λ_{max} (ϵ) = 305 (6500), 380 (sh) and 489 (1465).

Acknowledgements

The authors thank Dr. A. Deronzier (LEOPR, Grenoble) for fruitful discussions.

References

- (a) F. L. Carter, *Molecular Electronic Devices II*, Dekker, New York, 1987. (b) V. Balzani, M. Gomez-Lopez and J. F. Stoddart, *Acc. Chem. Res.*, 1998, **31**, 405.
- L. Zelikovich, J. Libman and A. Shanzer, *Nature*, 1995, **374**, 790.
- C. Canevet, J. Libman and A. Shanzer, *Angew. Chem., Int. Ed. Engl.*, 1996, **35**, 2657.
- S. Zahn and J. W. Canary, *Angew. Chem., Int. Ed. Engl.*, 1998, **37**, 305.
- C. Belle, G. Gellon, C. Scheer and J.-L. Pierre, *Tetrahedron Lett.*, 1994, **35**, 7019.
- J.-M. Lehn, *Supramolecular Chemistry*, VCH, Weinheim, Germany, 1995.
- M. Sano and H. Taube, *J. Am. Chem. Soc.*, 1991, **113**, 2327.
- M. Sano and H. Taube, *Inorg. Chem.*, 1994, **33**, 705.
- A. Livoreil, C. O. Dietrich-Buchecker and J.-P. Sauvage, *J. Am. Chem. Soc.*, 1994, **116**, 9399.
- G. De Santis, L. Fabbri, D. Iacopino, P. Pallavicini, A. Perotti and A. Poggi, *Inorg. Chem.*, 1997, **36**, 827.
- C. Belle, I. Gautier-Luneau, J.-L. Pierre, C. Scheer and E. Saint-Aman, *Inorg. Chem.*, 1996, **35**, 3706.
- J.-P. Gisselbrecht, M. Gross, J.-M. Lehn, J.-P. Sauvage, R. Ziessel, C. Piccini-Leopardi, J.-M. Arrieta, G. Germain and M. Van Meerse, *Nouv. J. Chim.*, 1984, **8**, 661.
- K. T. Potts, M. Keshavarz-K., F. S. Tham, H. D. Abruña and C. R. Arana, *Inorg. Chem.*, 1993, **32**, 4422.
- A. J. Bard and L. R. Faulkner, *Electrochemical Methods. Fundamentals and Applications*, John Wiley & Sons, New York, 1980.

Received in Montpellier, France, 27th July 1998;
Paper 8/05958F